Open access • Posted Content • DOI:10.1101/2021.05.07.443177

Mathematical Analysis and Topology of SARS-CoV-2, Bonding with Cells and Unbonding — Source link

Arni S.R. Srinivasa Rao, Steven G. Krantz

Institutions: Georgia Regents University, Washington University in St. Louis

Published on: 09 May 2021 - bioRxiv (Cold Spring Harbor Laboratory)

SHORT TITLE: TOPOLOGICAL ANALYSIS OF SARS-COV-2

Full title: Mathematical Analysis and Topology of SARS-CoV-2, Bonding with Cells and Unbonding

Arni S.R. Srinivasa Rao*,
Laboratory for Theory and Mathematical Modeling,
Medical College of Georgia,
Department of Mathematics,
Augusta University, Georgia, USA
email: arni.rao2020@gmail.com
*Corresponding author

Steven G. Krantz,
Department of Mathematics,
Washington University in St. Louis, Missouri, USA
email: sgkrantz@gmail.com

Abstract. We consider the structure of the novel coronavirus (SARS-Cov-2) in terms of the number of spikes that are critical in bonding with the cells in the host. Bonding formation is considered for selection criteria with and without any treatments. Functional mappings from the discrete space of spikes and cells and their analysis are performed. We found that careful mathematical constructions help in understanding the treatment impacts, and the role of vaccines within a host. Smale's famous 2-D horseshoe examples inspired us to create 3-D visualizations and understand the topological diffusion of spikes from one human organ to another organ. The pharma industry will benefit from such an analysis for designing efficient treatment and vaccine strategies.

Keywords: COVID-19, functional mapping, host cells, bonding, vaccines

1. Introduction

The structure of the virus and spikes of the novel coronavirus (SARS-CoV-2 or COVID-19) that caused the suffering during 2020-2021 is understood in this article through topological constructions. We showed how such careful visualizations help to understand the virus-cell bonding through the distribution of spikes of the SARS-CoV-2. In general, the number of spikes and distribution of the spikes across various virus particles is found to be key in the spread of SARS-CoV-2 [1, 2], bonding of the spikes [3, 4, 5], and in understanding the entry of the virus into key organs like the lungs [7, 8, 9, 10]. We found that such a detailed mathematical analysis will eventually assist in the careful design of vaccines and medicines. Several studies analyze the situations of inactivity of the SARS-CoV-2 and the role played by the spikes [11, 12, 13, 14, 15, 16].

Many experimental results on the spikes and their activation, bonding, and inactivation assisted in vaccine development [17, 18, 19]. The pharmaceutical and the vaccine industry would benefit from such detailed visualizations of internal structures and bonding, rate of unbonding, and the role of interventions [20, 21, 22, 23].

In spite of experimental success in identifying a set of vaccine candidates for SARS-CoV-2 and the activity of the spikes, there exist several uncertainties in measuring successful vaccine impact. Theoretically, if a spike is completely bonded by an infected cell and this bonding is executed perfectly then that should lead to a new virus. At the same time, preventing a successful bonding and breaking of the spike would leave the virus incapable of spreading. Experiments leading to the identification of spike structures and their activities need to be more accurate and our present theoretical analysis promises to be useful for assisting in the experiments. Pharmaceutical and vaccination industries need to conduct highly accurate laboratory experiments. These experiments would need to carefully understand the role played by the spikes in SARS-CoV-2. Vaccines are designed to destroy the bonding capacity of these spikes or even destroy the spikes. Mathematical mapping, identification, and analysis of the spikes responsible for virus production within a host that are analyzed in this article are highly insightful for such experiments.

Our article will assist in improved design of vaccine experiments and better treatment designs that can take care of all the spikes at the time of entry

into a host. Topological analysis is a rich tool and proper usage of it can help in avoiding uncertainties.

In this article, we have considered the following four assumptions in our topological constructions of the SARS-CoV-2:

- **(i)** Not all virus particles in the host are participating in infecting cells;
- **(ii)** Not all the spikes in a single virus may be bonded with cells;
- **(iii)** Each spike within a virus will bond with one and only cell;
- **(iv)** An empty spike (uninfected spike) of a given virus particle can bond with another cell.

This work provides original applications of topology which is one of the powerful tools of mathematical analysis [24, 25, 26, 27]. We cite here general references for the basic ideas of point-set topology. But our discrete constructions in this article are not explained in those sources. In the next section, we have described the basic topological space that we define using the number of spikes per virus particle within a host. We have provided novel usage of the mathematical analysis principles and topological constructions. A fraction of the spikes within a host in the space is allowed to get bonding with the uninfected cells. The entire structure of the space is mapped so that we can better understand the role of bonded and unbonded spikes within a host. Section 3 studies the role of treatment and vaccines in prohibiting the bonding and eliminating the infected host.

2. Topological Structures

Overall structure and topology of the virus and bonding/unbonding by cells within the host are described through Figure 2.2. Let $c_i^j(t_0)$ be the i^{th} novel coronavirus (ç) particle within a host at time t_0 that has j number of spikes. We choose $i = 1, 2, ..., n$ and $j = 1, 2, ..., j_i$. Each of the spikes within the host is uniquely identified by this structure because $\{c_1^1(t_0), c_1^2(t_0), ..., c_1^{j_1}(t_0)\}$ is the distinct set of spikes of the first virus particle and so on. In general, $\{c_i^1(t_0), c_i^2(t_0), ..., c_i^{j_i}(t_0)\}$ is the distinct set of spikes of the i^{th}-virus particle for $i = 1, 2, ..., n$.. Such a construction also allows us to write the expression:

$$\sum_{j=1}^{j_1} c_1^j(t_0) + \sum_{j=1}^{j_2} c_2^j(t_0) + \cdots + \sum_{j=1}^{j_i} c_i^j(t_0) + \cdots + \sum_{j=1}^{j_n} c_n^j(t_0) \tag{2.1}$$

The quantity $\Sigma_{i=1}^{n}\Sigma_{j=1}^{j_i} c_i^j(t_0)$ in (2.1) represents the total spikes in the host which are ready to bond with cells within the host. The spikes in the

expression (2.1) are not yet bonded. Let $S(t_0)$ be the collection of all the spikes which were not yet bonded at time t_0. Then

$$S(t_0) = \left\{ \left\{ \sum_{j=1}^{j_i} c_i^j(t_0) \right\} \text{ for } 1 \le i \le n, 1 \le j \le j_i \right\} \tag{2.2}$$

Let p_i be the fraction of the spikes in the i^{th}-virus particle which are bonded with uninfected cells at time t_1. The quantity $p_i = 1$ indicates that the i^{th} virus particle is fully bonded with uninfected cells, and each of the j_i spikes is occupied in bonding. The quantity $p_i < 1$ indicates that some of the spikes out of j_i spikes in the virus particle are unoccupied (or empty). We write

$$\sum_{i=1}^{n} p_i = \frac{\varphi(t_1)}{S(t_1)},$$

where $\varphi(t_1)$ is the total number of spikes in $S(t_1)$ which are bonded with uninfected cells at time t_1. The cardinality of the set $S(t_1)$ is

$$|S(t_1)| = \sum_{i=1}^{n} j_i.$$

When $p_i(t_1) = 1$ for all i, then $\varphi(t_1) = |S(t_1)|$ and when $p_i(t_1) < 1$ for at least one i, then $\varphi(t_1) < |S(t_1)|$. Suppose that $f_1 : S(t_0) \to S(t_1)$, where $S(t_1)$ consists of the set of all spikes both bonded and unbonded. The number of spikes that were bonded during $[t_0, t_1]$ is $p_i(t_1)j_i$ and $j_i - p_i(t_1)j_i$ is the number of spikes at t_1 which are not bonded with uninfected cells for $i = 1, 2, ..., n$. We assume an occupied spike with an uninfected cell will not be available for further bonding. So the bonded spikes at t_1, i.e., $p_i(t_1)j_i$, have completed their virus bonding capacity by time t_1, and the remaining spikes available at time t_1 are $j_i - p_i(t_1)j_i$. These unbonded spikes will be available for bonding during $(t_1, t_2]$. Let d_i^k be the k^{th} bonded spike at time t_1 out of j_i spikes at time t_0 for $k = 1, 2, ..., p_i(t_1)j_i$ such that

$$\sum_{k=1}^{p_i(t_1)j_i} d_i^k + \sum_{j=1}^{j_i - p_i(t_1)j_i} c_i^j = j_i \text{ for } i = 1, 2, ..., n. \tag{2.3}$$

The number of occupied spikes among all the virus particles during $[t_0, t_1]$ which will not be available for further bonding are

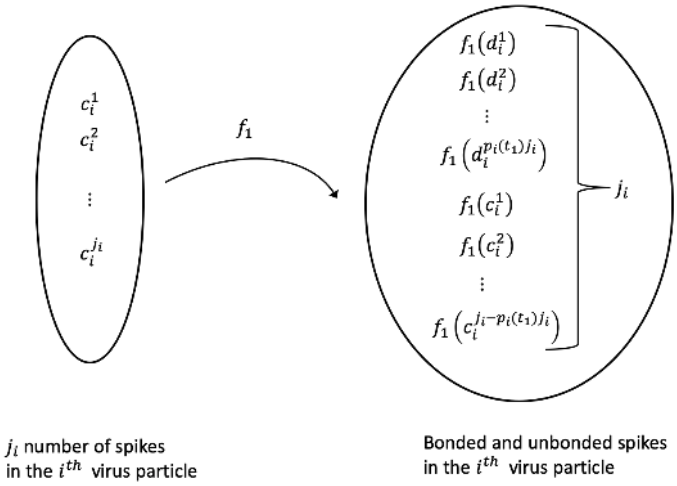

FIGURE 2.1. Mapping of spikes in the i^{th} virus particle at time t_0 to bonded and unbonded spikes at time t_1.

$$\sum_{i=1}^{n} \sum_{k=1}^{p_i(t_1)j_i} d_i^k$$

If $p_i(t_1) = 1$ for any i at time t_1 then that virus particle has completed the bonding role in the system. It is assumed that $p_i(t_1)j_i$ number of spikes for each i (when $p_i(t_1) < 1$) would generate $p_i(t_1)j_i$ number of new virus particles available for bonding during $[t_0, t_1]$, else (when $p_i(t_1) = 1$) it would generate j_i number of new virus particles during the same period. See Figure 2.1.

Hence the newer virus particles produced during $[t_0, t_1]$ are $\sum_{i=1}^{n} p_i(t_1)j_i$, so the available virus particles for bonding at time t_1 will be

$$n + \sum_{i=1}^{n} p_i(t_1)j_i \qquad (\text{if } p_i(t_1) < 1 \ \forall i)\,. \tag{2.4}$$

The birth rate $\lambda_i(t_1)$ $(w.r.t.\ n)$ of the new virus particles during $[t_0, t_1]$ is

$$\lambda_i(t_1) = \frac{\sum_{i=1}^{n} p_i(t_1)j_i}{n}\,. \tag{2.5}$$

Not all of the new viruses at time t_1 in (2.4) may be available for bonding during $(t_1, t_2]$ if one or more of the virus particles (out of n) might have all its spikes bonded at time t_1.

Suppose that $p_{i'}(t_1)j_{i'} = j_{i'}$ for $i' = 1, 2, ..., m$ $(m < n)$ and $p_{i*}(t_1)j_{i*} < j_{i*}$ for $i* = 1, 2, ..., n - m$, such that

$$\sum_{i'=1}^{m} j_{i'} + \sum_{i*=1}^{n-m} j_{i*} = \sum_{i=1}^{n} j_i. \tag{2.6}$$

Based on (2.6), the number of virus particles available at time t_1 after removing completely bonded virus particles during $[t_0, t_1]$ (i.e., those virus particles for which all of its spikes were bonded with uninfected cells, and adding new virus particles created by the $n-m$ virus particles with available spikes for bonding during $[t_0, t_1]$) are

$$n + \sum_{i*=1}^{n-m} j_{i*} - \sum_{i'=1}^{m} j_{i'}. \tag{2.7}$$

The total number of bonded spikes due to $\sum_{i*=1}^{n-m} j_{i*}$ and $\sum_{i'=1}^{m} j_{i'}$ are

$$\sum_{i*=1}^{n-m} p_{i*}(t_1)j_{i*} + \sum_{i'=1}^{m} p_{i'}(t_1)j_{i'} = \sum_{i*=1}^{n-m} p_{i*}(t_1)j_{i*} + \sum_{i'=1}^{m} j_{i'}, \tag{2.8}$$

and, from (2.3),

$$\sum_{i*=1}^{n-m} p_{i*}(t_1)j_{i*} + \sum_{i'=1}^{m} j_{i'} = \sum_{k=1}^{p_i(t_1)j_i} d_i^k \tag{2.9}$$

Let us decompose $\sum_{k=1}^{p_i(t_1)j_i} d_i^k$ as

$$\sum_{k=1}^{p_i(t_1)j_i} d_i^k = \sum_{i*=1}^{n-m} a_{i*} + \sum_{i'=1}^{m} b_{i'}, \tag{2.10}$$

where $a_{i*} = p_{i*}(t_1)j_{i*}$ and $b_{i'} = j_{i'}$.

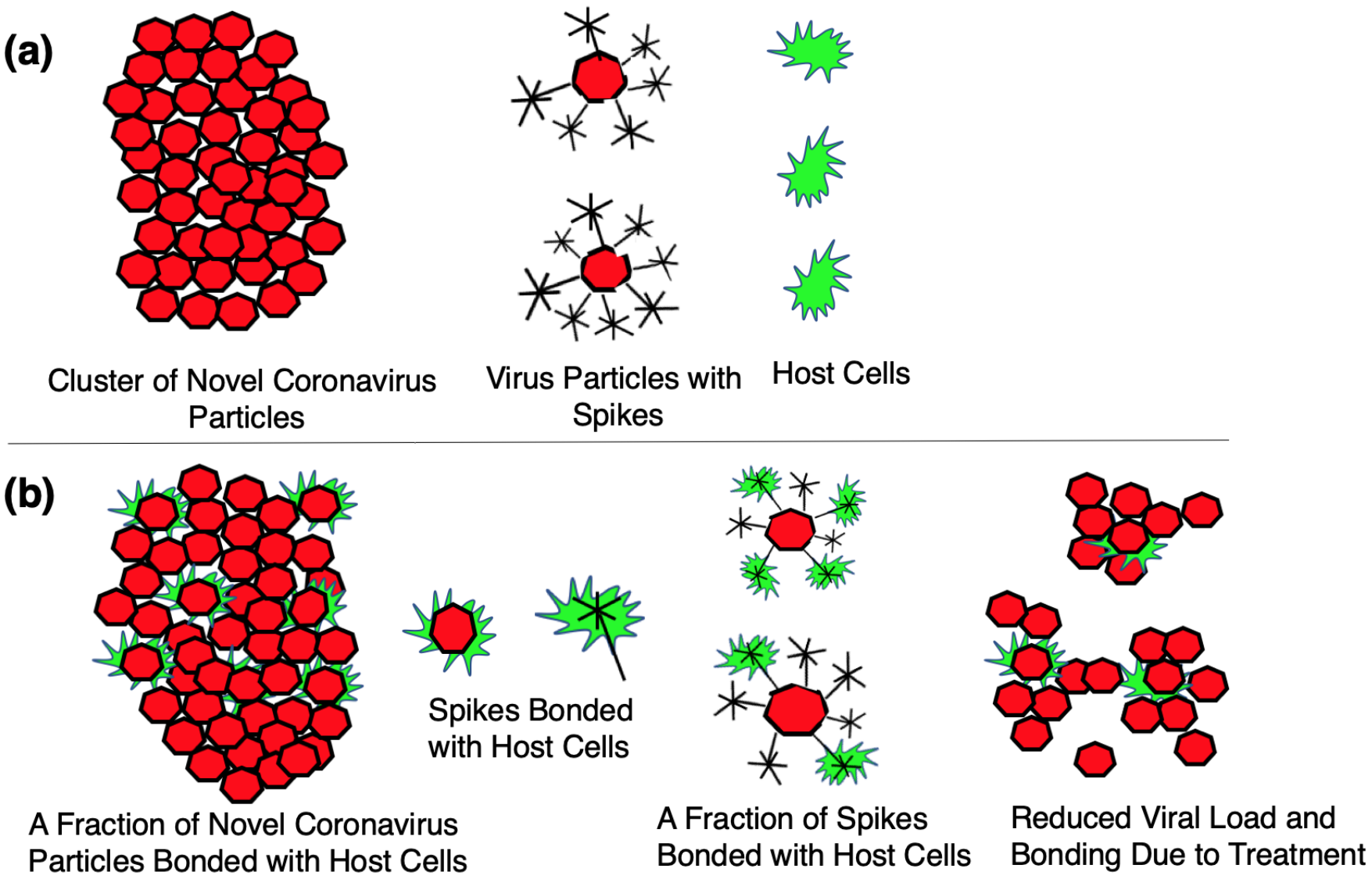

FIGURE 2.2. Topology of novel coronavirus (SARS-CoV-2), spikes, bonding, reduction in virus bonding due to treatment. (a) Imaginative description of the SARS-CoV-2, spikes and host cells, (b) Bonding of spikes to host cells, reduction of viral load due to treatment.

The total bonded during $[t_0, t_2]$ is responsible for giving birth to new viruses as described previously. The total number of remaining spikes, those $|S(t_1)|$ which are available at time t_1, are the sum of (i) the number of spikes unbonded during $[t_0, t_1]$, and (ii) the number of spikes that are created due to the birth of new virus particles. The listing of the set $S(t_1)$ of spikes helps in constructing the function $f_2 : S(t_1) \to S(t_2)$. Here $S(t_2)$ is the set of spikes created by $S(t_1)$ during $(t_1, t_2]$. Let us list the elements of the set $S(t_1)$ below:

The list of unbounded spikes J_1 during $[t_0, t_1]$ is obtained as remaining spikes from the first term of (2.9) as

$$\{\{j_i - a_{i*}\} \text{ for } i* = 1, 2, ..., n - m\} \,. \tag{2.11}$$

The list of spikes A_1 available at $S(t_1)$ because of the first term of the R.H.S. of (2.10) is

$$\left\{\{a_1^1, ..., a_1^{a_1}\}, \{a_2^1, ..., a_2^{a_2}\}, ..., \{a_{n-m}^1, ..., a_{n-m}^{a_{n-m}}\}\right\}, \tag{2.12}$$

where the a_i^j in (2.12) represent the j^{th} spike of the i^{th} virus resulting from $\sum_{i*=1}^{n-m} a_{i*}$ in (2.10). That is, as per the set in (2.12), there are a_1 number of spikes for the first virus, a_2 numbr of spikes for the second virus, and so on a_{n-m}spikes for the $(n-m)^{th}$ virus. The list of spikes B_1 available at $S(t_1)$ due to the resultant of the second term of the R.H.S. of (2.10) is

$$\left\{\{b_1^1, ..., b_1^{b_1}\}, \{b_2^1, ..., b_2^{b_2}\}, ..., \{b_m^1, ..., b_m^{b_m}\}\right\}, \tag{2.13}$$

where the b_i^j in (2.13) represent the j^{th} spike of i^{th} virus resulting out of $\sum_{i'=1}^{m} b_{i'}$ in (2.10). That is, as per the set in (2.13), there are b_1 number of spikes for the first virus, b_2 numbr of spikes for the second virus, and so on b_m spikes for the m^{th} virus. The domain $S(t_1)$ of the function f_2 will have the collection of all the elements of the sets J_1, A_1 and B_1, i.e.

$$S(t_1) = J_1 \cup A_1 \cup B_1 \,. \tag{2.14}$$

The collections $S(t_0)$ and $S(t_1)$ constructed above can be treated as two spaces and $S(t_1)$ in (2.14) is now seen as a disconnected space.

Lemma 1. *The function f_1 is not* 1–1 *when bonding occurs during* $[t_0, t_1]$.

Proof. We have $f_1 : S(t_0) \to S(t_1)$, where $S(t_0)$ and $S(t_1)$ are the sets of all the distinct spikes at time t_0 and time t_1. When bonding occurs during $[t_0, t_1]$, the set of all spikes at time t_1 will be $S(t_1)$ as seen in (2.14). This implies that

$$|S(t_1)| = |J_1 \cup A_1 \cup B_1|$$

$$= |J_1| + |A_1| + |B_1|$$

From (2.11) to (2.13) we can write

$$|J_1| + |A_1| + |B_1| > \sum_{i=1}^{n} j_i = S(t_0) \tag{2.15}$$

Because of the inequality (2.15), f_1 cannot be 1–1. □

Corollary 2. *The function f_1 is 1–1 when no bonding occurs during $[t_0, t_1]$. When the bonding does not occur then $|S(t_0)| = |S(t_1)|$ and the elements of $S(t_0)$ and $S(t_1)$ are not different.*

Since we can consider

$$S(t_0) = \bigcup_{i=1}^{n} \bigcup_{j=1}^{j_i} \left\{ c_i^j \right\}$$

and the elements of $s(t_0)$ are distinct, we treat here $S(t_0)$ as a discrete topological space with $|S(t_1)| = \sum_{i=1}^{n} j_i$ elements in the space $S(t_0)$. Let $S_X(t_0)$ and $S_Y(t_1)$ be two subsets of $S(t_0)$ such that $S_X(t_0)$ represents bonded spikes and $S_Y(t_0)$ represents unbonded spikes during $[t_0, t_1]$. Then, by the construction of $S(t_0)$, the two subsets $S_X(t_0)$ and $S_Y(t_0)$ form two disjoint subspaces of $S(t_0)$. The space $S(t_1)$ as well is a discrete topological space and three subsets of it J_1, A_1 and B_1, form three disjoint topological discrete subspaces of $S(t_1)$.

Definition 3. Topological diffusion: We define here the topological diffusion $D_s(t_0)$ of the space created due to newer spikes during $[t_0, t_1]$, as

$$D_s = (S(t_0) \cup S(t_1)) \setminus S(t_0)\,. \tag{2.16}$$

Theorem 4. *The topological diffusion $D_s(t_0)$ during $[t_0, t_1]$ is $A_1 \cup B_1$.*

Proof. We have

$$D_s = (S(t_0) \cup S(t_1)) \setminus S(t_0) \tag{2.17}$$

The set $D_s(t_0)$ indicates the newer elements created in the combined space $(S(t_0) \cup S(t_1))$. The collection of elements of $S(t_0)$ and $S(t_1)$ in (2.17) are further expressed using (2.14) as follows:

$$\begin{aligned}
&= (S_X(t_0) \cup S_Y(t_0)) \cup (J_1 \cup A_1 \cup B_1) \setminus (S_X(t_0) \cup S_Y(t_0)) \\
&= S_X(t_0) \cup J_1 \cup A_1 \cup B_1 \setminus (S_X(t_0) \cup S_Y(t_0)) \\
&= J_1 \cup A_1 \cup B_1 \setminus S_Y(t_0) \\
&= A_1 \cup B_1
\end{aligned}$$

□

The collection $A_1 \cup B_1$ is the newer space created during $[t_0, t_1]$.

Example 5. Suppose $S(t_0)$ has 10 spikes. The topological diffusion occured during $[t_0, t_1]$ to arrive at $|S(t_1)| = 21$. See Figure 2.3 for mapping of bonded cells into new spikes and carrying forward the unbonded spikes.

Every singleton set within $S(t_0)$ is an open subset. That means that each spike in $S(t_0)$ is considered as a singleton set and $S_X(t_0)$ and $S_Y(t_0)$ form two open subsets of $S(t_0)$. In fact, according to discrete topology $S_X(t_0)$ and $S_Y(t_0)$ can also be treated as closed subsets (so the space is disconnected). The transformations of the space $S(t_0)$ during $[t_0, t_1]$ would lead to newer spaces due to bonding (also argued as in the proof of Lemma 1). Such a creation of new topological spaces and their cardinality can be influenced with a treatment intervention at some time t for $t \in [t_0, t_1]$. Treatment works in reducing the value of p_i or the death rates of the virus particles c_i^j or both.

3. Treatment and Vaccinations

We assume a treatment to kill the virus population (viral load within a host) would increase the mortality rate of the virus population and reduce the bonding of the uninfected cell population with SARS-CoV-2. At time t_0 the viral load would be lower and treatment during $[t_0, t_1]$ would have a higher impact on reducing the viral load than if the treatment was introduced

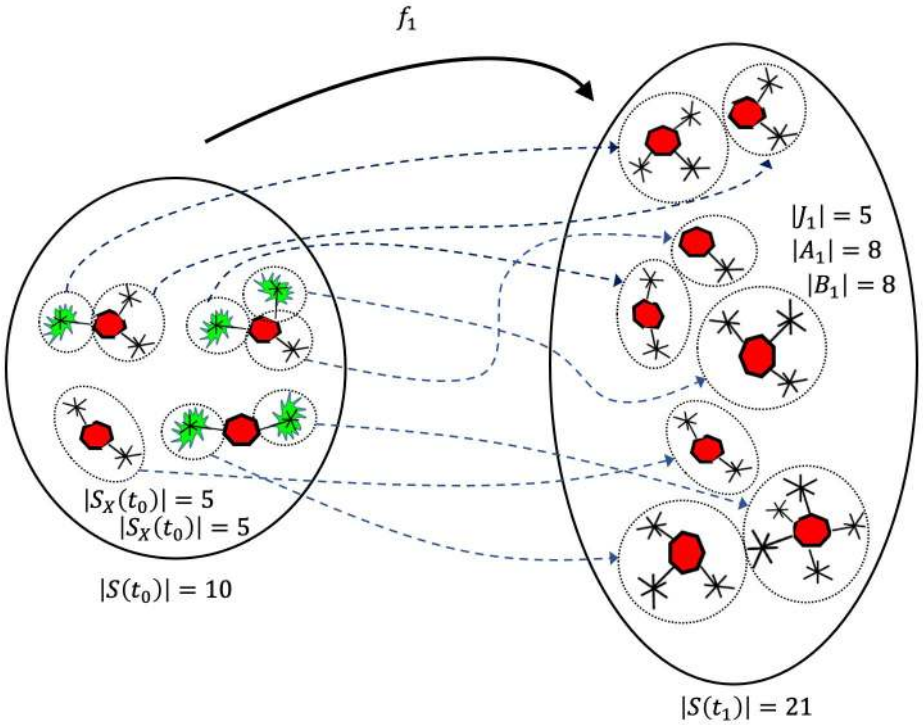

FIGURE 2.3. Numerical example of mapping of bonded and unbonded spikes. $A_1 \cup B_1 = 16$ as shown is the topological diffusion of the space.

during $[t_1, t_2]$. We assume a longer time to introduce a treatment after time t_0 according to the longer time the virus population is restricting the virus growth. Since $|S(t_0)| < |S(t_1)|$ in the absence of treatment, $S(t_0) = S(t_1)$ can be achieved (Corollary 2) when treatments are introduced during $[t_1, t_2]$. We assume the host will be dominated by the virus when virus growth is not controlled and the virus will be eliminated either naturally or due to treatment impact. Let p_i be defined as earlier and let $q_i(t_1)$ be the fraction of the spikes in the i^{th} virus which are bonded during $[t_0, t_1]$ and treatment was introduced at some time s for $s \in (t_0, t_1]$. Here, $0 \leq q_i(t_1) < p_i(t_1)$. The quantity $q_i(s) = 0$ means there are no bonded spikes at s. The quantity $q_i(s)$ would never reach $p_i(t_1)$. Since the treatment would also increase the mortality rate of the c_i^j population, we assume that $q_i(t_1) = 0$ if i^{th} virus dies at s for $s \in (t_0, t_1]$ or $q_i(t_1) = 0$ if no bonding with the spikes of the i^{th} virus occurs. When $q_i(t_1) = 0$, then all the spikes of the i^{th} virus at t_0 will be available for bonding during $(t_0, t_1]$.

Theorem 6. *Consider the sequence of functions* $(f_n)_{n\geq 1}$*, where* $f_n : S(t_{n-1}) \to S(t_n)$*. Suppose a treatment is introduced at* t_m *for some* $m \geq 1$*. Then the sizes of* $S(t_i)$ *are increasing until* t_m *and the sizes of* $S(t_i)$ *are decreasing until* $S(t_{m-1})$ *and* $f_m : S(t_{m-1}) \to \phi$ *(empty set).*

Proof. When treatment prohibits bonding then virus population having no host would eventually die. Treatment would also kill bonded cells with spikes. Suppose the treatment is introduced at time s for $s > t_0$ and

$$s \in \{t_0, t_1, ...t_m, ...\}.$$

The time intervals were partitioned as $\{[t_0, t_1], (t_1, t_2], ..., \}$. Given that $s = t_m$, we assume impact of the treatment can be measured in prohibiting the bonding at t_m for $m > 0$. Similarly the treatment would have impact on killing the bonded cells with spikes at t_m. Hence

$$|S(t_0)| < |S(t_1)| < ... < |S(t_{m-1})| \tag{3.1}$$

and

$$|S(t_{m-1})| > |S(t_m)| > |S(t_{m+1})| > ... \tag{3.2}$$

The sequence $S(t_{m-1})_{m\geq 1}$ in (3.2) is monotonic and $0 \leq |S(t_m)|$ for all $m \geq 0$. Hence, by the monotone convergence theorem, the sequence (3.2) is convergent to ϕ (empty set). □

Theorem 7. *Consider the sequence of functions* $(f_n)_{n\geq 1}$*, where* $f_n : S(t_{n-1}) \to S(t_n)$*. Suppose the host is vaccinated prior to* t_0*. Then the sequence* $S(t_m)_{m\geq 0}$ *is decreasing and* $lim_{n\to\infty} |S(t_m)| = 0$*.*

Proof. Given $f_n : S(t_{n-1}) \to S(t_n)$ for all n. When the host is vaccinated prior to t_0 the system will prohibit the spikes to get bonded with cells. Unbounded spikes and virus particles dying over time lead to the decreasing sequence

$$|S(t_0)| > |S(t_1)| > ... > |S(t_m)| > \cdots . \tag{3.3}$$

Similar to the argument of the proof of the Theorem 6, we have

$$\lim_{n\to\infty} |S(t_m)| = 0. \tag{3.4}$$

□

Remark 8. A vaccinated host would alter the range of f_1 in Example 5 but the domain of f_1 consisting of vaccinated and not vaccinated hosts remains the same. COVID-19 vaccinations would not prevent virus to enter an unprotected host, but a vaccinated host prevents the virus from getting bonded with the virus spikes.

Given Theorem 7, this sequence of inequalities will emerge:

$$|S(t_0)| - |S(t_1)| = \sum_{i=1}^{n} \kappa_{1_i} > 0$$
$$|S(t_1)| - |S(t_2)| = \sum_{i=1}^{n} \kappa_{2_i} > 0$$
$$\vdots$$
$$|S(t_{m-1})| - |S(t_m)| = \sum_{i=1}^{n} \kappa_{m_i} > 0$$
$$\vdots$$

Since (3.4) is true, we will have

$$|S(t_n)| - |S(t_{n+1})| \to 0 \text{ as } n \to \infty.$$

Here κ_{m_i} for $m = 1, 2, ...$ is the remaining number of spikes unbounded during $[t_{i-1}, t_i]$ for $i = 1, 2, ..., n$. We can create the elements similar to (2.11) to (2.13) for the periods $\{[t_0, t_1], (t_1, t_2], ..., \}$. Let J_τ, A_τ, B_τ be the sets defined on the intervals $\{[t_0, t_1], (t_1, t_2], ..., \}$ similar to J_1,A_1,B_1 which were defined from (2.11) to (2.13) for the emenets defined on the interval $[t_0, t_1]$. The topological diffusion created until the treatment initiated at t_m is $\bigcup_{\tau=1}^{m-1} A_\tau \cup B_\tau$. Hence the diffusion of the elements created will start declining with the initiation of the treatment. The smaller the value of t_m, the lesser the quantity $\bigcup_{\tau=1}^{m-1} A_\tau \cup B_\tau$.

Theorem 9. *Topological structures of the virus populations and spikes will be different under vaccination and treatment of hosts even though* $|S(t_n)| - |S(t_{n+1})| \to 0$ *as* $n \to \infty$.

Proof. Suppose the treatment is initiated within a host at t_m for $m \geq 1$. The topological structure of spikes would first have the increasing property in (3.1), and then will start decreasing as in (3.2). This leads to $|S(t_n)| - |S(t_{n+1})| \to 0$ as $n \to \infty$.

Under a vaccinated host, as soon as the SARS-CoV-2 virus enters at t_0, the topological structure of the spike population spread within the host obeys (3.3), and that leads to $|S(t_n)| - |S(t_{n+1})| \to 0$ as $n \to \infty$.

Hence, two topological structure described above will be different although the limiting number of spikes diminishes. □

3.1. **Horseshoe mapping.** Inspired by Stephen Smale's original famous *horseshoe* example [28, 30, 31], we have visualized a discretized version of the same idea with plastic beads in a container. Let us consider a hollow cube and fill it with plastic beads. Suppose all the beads in this cube are transferred into a horseshoe-shaped pipe. See Figure 3.1. Note that the original horseshoe mapping is continuous and is a diffeomorphism between a square and horseshoe-shaped space. Let us imagine the size of the $S(t_1)$ SARS-CoV-2 spikes are located in the throat area of a human host. Suppose during the interval $(t_1, t_2]$ these spikes are spread into the lung area. Assume that the treatment to control the virus is initiated at t_2 such that the throat area spikes are eliminated during $(t_2, t_3]$ and the number of spikes at t_3, is the set $S(t_3)$. This leads to

$$|S(t_1)| = |S(t_3)|\,.$$

Transformation of the number of spikes of $S(t_1)$ in the throat area into number of spikes of lungs area is demonstrated in Figure 3.2. Suppose the size of the spikes at t_1 are located in the throat area of a host. We have $f_1 : S(t_0) \to S(t_1)$. Under the no treatment assumption during $(t_1, t_2]$, we have $f_2 : S(t_1) \to S(t_2)$, where $|S(t_2)| > |S(t_1)|$. The newer space created during $(t_1, t_2]$ is

$$A_2 \cup B_2. \tag{3.5}$$

The topological diffusion in (3.5) gives us,

$$\begin{aligned} S(t_2) &= S(t_1) \cup A_2 \cup B_2 \\ &= J_1 \cup (A_1 \cup A_2) \cup (B_1 \cup B_2)\,. \end{aligned}$$

Suppose the treatment for SARS-CoV-2 is introduced at t_2 such that

$$|S(t_2)| > |S(t_3)| \tag{3.6}$$

is attained. There are now three possibilities that will arise due to (3.6):

$$\text{(i)}\, |S(t_3)| > |S(t_1)|$$

$$\text{(ii)}\, |S(t_3)| = |S(t_1)|$$

$$\text{(iii)}\, |S(t_3)| < |S(t_1)|$$

Above possibility (ii) we associate with that of Smale's *horseshoe* type of example and is also demonstrated in Figure 3.2. During $(t_2, t_3]$ the number of spikes killed in the throat due to the treatment initiated at t_2 and due to the creation of the topological diffusion $A_2 \cup B_2$ reaches the size $|S(t_1)|$ at t_3. Then this kind of discrete topological transformation of the number of spikes at t_1 into the number of spikes at t_3 in a different location of a host is topologically visualized as an *horseshoe* type of example. Of course, we are aware in a true sense Smale's *horseshoe* is a diffeomorphism between two open spaces (a square and a a horseshoe). The current analysis of transformations of the number of spikes located at t_1 in the throat area and the number of spikes at t_3 in the lungs within a host handles the points (elements) of the space discretely.

The horseshoe example transforms the points of an open square into an equivalent area horseshoe using continuous mapping. The implications of the horseshoe are plenty—for example, the squeezing and stretching of a square to a horseshoe-shaped space in the creation of hyperbolic dynamics and chaos. In our analogy, the spikes in the throat within a human host do not get transferred to the lungs because virologically spikes do not travel within the host but they grow over time under a no-treatment scenario. Only after treatment is initiated are the spikes in the throat killed and an equivalent number of newer spikes born to remain active for some time in the lungs. We imagine this phenomenon as described through Figure 3.2 as the transformation of spikes of the throat to that of the lungs.

The geometry of the horseshoe is especially meaningful for us because spikes from the throat area due to the initial infected virus population are all located in one place. Then, due to the spread of the virus over the

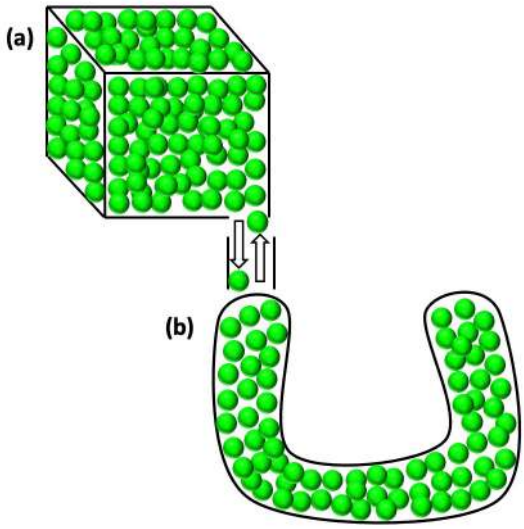

FIGURE 3.1. Transformation of a cube containing beads into a horseshoe-shaped pipe containing the same number of beads. **(a)** A cube container of green color beads, **(b)** Beads in **(a)** are transferred into a horseshoe shaped pipe. The number of beads in **(a)** and **(b)** are equal. The beads in **(b)** can be transferred into **(a)**. The beads occupying capacities of containers in **(a)** and **(b)** are equal and it is assumed that no free space left to add an additional bead into these containers. The original example of Stephen Smale is a diffeomorphism between two 2-D objects, namely, a square and a horseshoe, famously known as Smale's *horseshoe*.

intervals $\{[t_0, t_1], (t_1, t_2], ..., \}$, they diffuse into different organs which have geometrically a different shape than the throat. With the example of beads (Figure 3.1), and assuming no scope for adding a new bead in the cube, the corresponding pipe would take the 2D horseshoe to a 3D similar-shaped pipe through discrete topology. Our spikes analogy is that the horseshoe example was built on 2D and diffusion of spikes within the human organs is imagined in 3D.

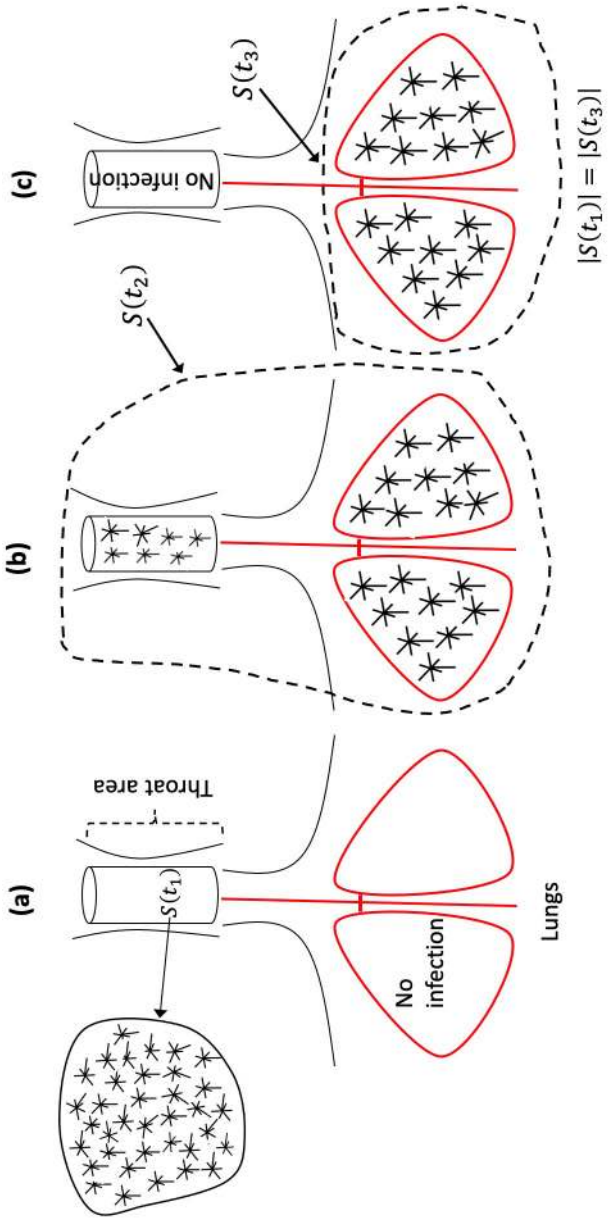

FIGURE 3.2. Transformation of the number of spikes at t_1 in the throat area into the number of spikes at t_3 in the lungs area. (a) The number of spikes in the throat at t_1 are $S(t_1)$ and no infection in lungs, (b) The number of spikes grown during $(t_1, t_2]$ expanded into lungs and treatment is introduced at t_2, (c) The spikes in the throat are killed and the number of spikes at t_3 in the lungs are $S(t_3)$ and $|S(t_1)| = |S(t_3)|$.

4. Discussion

Our study provides the most accurate mathematical structuring of the space of the SARS-CoV-2 virus and its spikes within the host. See the expression $S(t_0) = \left\{\left\{\sum_{j=1}^{j_i} c_i^j(t_0)\right\} \text{ for } 1 \leq i \leq n, 1 \leq j \leq j_i\right\}$ in section 2 and the clustering of spikes into bonded and unbonded spikes. The advantage of such a structure is to provide a detailed scope for mapping a spike that is available for bonding with an uninfected cell. Not a single unbonded spike will be left out in this process. The procedure also helps in tracking a bonded virus in such a way that the birth of newer virus particles through bonded spikes is monitored. See the expression $S(t_1) = J_1 \cup A_1 \cup B_1$, where J_1, A_1, and B_1 form three disjoint topological discrete subspaces mapped out from $S(t_0)$. The set J_1 emerges out of unbonded spikes in a previous time point and $A_1 \cup B_1$ is the collection of spikes generated due to bonding spikes with cells at a previous time point. Our clear-cut visualization of the theoretical constructions helps in understanding the structure of the spike-cells within the space.

Laboratory experiments on the virus particles and bonding are usually done on a group of viruses. Our procedure provides deeper insight for better design in conducting experiments on isolated individual viruses. Such a method will help in aggregating the virus population along with their number of spikes and measuring bonded and unbonded spikes for each virus particle. Lemma 1 provides the growth of spikes and their mapping of initial spikes that can create newer spaces within a time interval.

One of the central features of our construction is the development of a new measure that we call "*topological diffusion*." In general topology, no such measure exists. Using this measure, one can study the growth of spikes over time. The topological diffusion introduced in this article not only identifies the new spikes that emerge but how many of those were due to virus particles that had partial bonding of the spikes. These novel ideas make our work more practically implementable in pharmaceutical and vaccine industrial experiments. We have theoretically established this value within a small interval $A_1 \cup B_1$ and also over a large interval. The descriptions of A_1 and B_1 are recorded in previous paragraphs and also in section 2. Figure 2.3 provides an example of measuring the topological diffusion.

Theorem 6 provides the impact of a treatment in eliminating virus particles and Theorem 7 provides the impact of the vaccine on eliminating viruses

after entry into a host. We also generalize our results over multiple time intervals and the timing of initiation of therapy. Topological diffusion constructed in the article is also associated with Stephen Smale's famous horseshoe type of example. The original example by Smale was constructed as a diffeomorphism of two open spaces, namely, a square and corresponding sized area of a horseshoe. However, the current article considered a transformation of a discrete collection of spikes in one organ of a human host into the equivalent number of spikes in a different organ. Moreover, the demonstration we provided was between two 3-D shaped organs within a human host. Such visualization of the horseshoe example is new in the literature.

Concluding Remarks

The study presented in this paper is original and incisive. It uses powerful mathematical techniques—most notably ideas from topology—to analyze the bonding of corona virus cells. Our emphasis on discrete topology is somewhat novel.

As a result we obtain insights that will be useful in the production of new and more effective vaccines. We believe that the use of mathematical analysis in a medical context is a new and effective technique for epidemiology that will become recognized and solidly established in future work.

References

[1] Choe, H. and Farzan, M (2021). How SARS-CoV-2 first adapted in humans, *Science*, 372 (6541) Pages 466-467. Doi 10.1126/science.abi4711

[2] Hoffmann M. et al (2020). SARS-CoV-2 cell entry depends on ACE2 and TMPRSS2 and is blocked by a clinically proven protease inhibitor. *Cell.* 2020;181:271–80.e8.

[3] Zhang J et al (2021). Structural impact on SARS-CoV-2 spike protein by D614G substitution, *Science*, Vol. 372, Issue 6541, pp. 525-530 DOI: 10.1126/science.abf2303.

[4] Berger, I., Schaffitzel, C. The SARS-CoV-2 spike protein: balancing stability and infectivity. *Cell Res* 30, 1059–1060 (2020). https://doi.org/10.1038/s41422-020-00430-4

[5] Hussain, M, Jabeen, N, Raza, F, et al. Structural variations in human ACE2 may influence its binding with SARS-CoV-2 spike protein. *J Med Virol.* 2020; 92: 1580–1586. https://doi.org/10.1002/jmv.25832

[6] Greaney A.J. et al (2021). Complete Mapping of Mutations to the SARS-CoV-2 Spike Receptor-Binding Domain that Escape Antibody Recognition, *Cell Host & Microbe* Volume 29, Issue 1, 13 January 2021, Pages 44-57.e9

[7] Bangaru, S et al (2021). Structural analysis of full-length SARS-CoV-2 spike protein from an advanced vaccine candidate. *Science* 370, 1089–1094 (2020). doi:10.1126/science.abe1502pmid:33082295

[8] Walls, A. C. et al. Structure, function, and antigenicity of the SARS-CoV-2 spike glycoprotein. *Cell* https://doi.org/10.1016/j.cell.2020.02.058 (2020).

[9] Y. Cai, J. Zhang, T. Xiao, H. Peng, S. M. Sterling, R. M. Walsh Jr.., S. Rawson, S. Rits-Volloch, B. Chen, Distinct conformational states of SARS-CoV-2 spike protein. *Science* 369, 1586–1592 (2020).

[10] Huilan Zhang, Peng Zhou, Yanqiu Wei, et al. Histopathologic Changes and SARS-CoV-2 Immunostaining in the Lung of a Patient With COVID-19. *Ann Intern Med.*2020;172:629-632. [Epub ahead of print 12 March 2020]. doi:10.7326/M20-0533

[11] Liu, C et al (2021). The Architecture of Inactivated SARS-CoV-2 with Postfusion Spikes Revealed by Cryo-EM and Cryo-ET. *Structure* 28, 1218–1224.e4 (2020). doi:10.1016/j.str.2020.10.001pmid:33058760

[12] Petruk G et al (2020). SARS-CoV-2 spike protein binds to bacterial lipopolysaccharide and boosts proinflammatory activity, *Journal of Molecular Cell Biology*, 12, (12), 2020, Pages 916–932, https://doi.org/10.1093/jmcb/mjaa067

[13] Patra T et al (2020). SARS-CoV-2 spike protein promotes IL-6 trans-signaling by activation of angiotensin II receptor signaling in epithelial cells, *PLOS Pathogens*, https://doi.org/10.1371/journal.ppat.1009128

[14] Herrera N.G. et al (2021). Characterization of the SARS-CoV-2 S Protein: Biophysical, Biochemical, Structural, and Antigenic Analysis. *ACS Omega*, 6, 1, 85–102 Publication Date:December 21, 2020 https://doi.org/10.1021/acsomega.0c03512

[15] Guruprasad, L. Human SARS CoV-2 spike protein mutations. *Proteins.* 2021; 89: 569– 576. https://doi.org/10.1002/prot.26042

[16] Srivastava, S, et. al. (2020) Computationally validated SARS-CoV-2 CTL and HTL Multi-Patch vaccines, designed by reverse epitomics approach, show potential to cover large ethnically distributed human population worldwide, *Journal of Biomolecular Structure and Dynamics,* DOI: 10.1080/07391102.2020.1838329

[17] Watanabe, Y. et al. (2021) Native-like SARS-CoV-2 Spike Glycoprotein Expressed by ChAdOx1 nCoV-19/AZD1222 Vaccine. *ACS Central Science,* https://doi.org/10.1021/acscentsci.1c00080

[18] Choi B Choudhary MC Regan J et al. Persistence and evolution of SARS-CoV-2 in an immunocompromised host. *N Engl J Med*. 2020; (published online Nov 11.) https://doi.org/10.1056/NEJMc2031364

[19] Krammer, F. SARS-CoV-2 vaccines in development. *Nature* 586, 516–527 (2020). https://doi.org/10.1038/s41586-020-2798-3

[20] Ismail, S, Ahmad, S, Azam, S. S (2020). Immunoinformatics characterization of SARS-CoV-2 spike glycoprotein for prioritization of epitope based multivalent peptide vaccine. *Journal of Molecular Liquids,* 314 Pages 113612

[21] Kar, T., Narsaria, U., Basak, S. et al. A candidate multi-epitope vaccine against SARS-CoV-2. *Sci Rep* 10, 10895 (2020). https://doi.org/10.1038/s41598-020-67749-1

[22] Sanders JM, Monogue ML, Jodlowski TZ, Cutrell JB (2020). Pharmacologic treatments for coronavirus disease 2019 (COVID-19): a review. *JAMA*. 2020;323:1824–36.

[23] Dharma K. et al. (2020). COVID-19, an emerging coronavirus infection: advances and prospects in designing and developing vaccines, immunotherapeutics, and therapeutics. *Hum Vaccin Immunother.* 2020;16:1232–8

[24] Munkres, James R. *Topology* (2/e). Prentice Hall, Inc., Upper Saddle River, NJ, 2000. xvi+537 pp. ISBN: 0-13-181629-2

[25] Krantz, S. G (2010) *Essentials of topology with applications*. Textbooks in Mathematics. CRC Press, Boca Raton, FL, 2010. xvi+404 pp. ISBN: 978-1-4200-8974-5

[26] Singh, T. B (2019) *Introduction to topology*. Springer, Singapore, 2019. xix+452 pp. ISBN: 978-981-13-6953-7; 978-981-13-6954-4

[27] Sakai, K (2013). *Geometric aspects of general topology*. Springer Monographs in Mathematics. Springer, Tokyo, 2013. xvi+521 pp. ISBN: 978-4-431-54396-1; 978-4-431-54397-8

[28] Smale, S. (1967). Differentiable dynamical systems. *Bull. Amer. Math. Soc.* 73 (1967), 747–817.

[29] Smale, S (1998). Finding a horseshoe on the beaches of Rio, *Mathematical Intelligencer* 20 (1998), 39-44.

[30] Shub, M (2005). What is a Horseshoe?, *Notices of the AMS*, v.52, p.530-532

[31] Ruelle, D (2006). What is ... a strange attractor? *Notices of the AMS*. 53, no. 7, 764–765.